Design of Machines and Structures, Vol4, No. 2 (2014) pp. *35–44*.
https://doi.org/10.32972/dms.2014.016

MESOSCOPIC LATTICE-BOLTZMANN MODELLING OF FLOW IN THIN CHANNEL WITH ROUGH WALLS

VALERY POROSHIN–DMITRY BOGOMOLOV–ANNA ANOSOVA–
VICTOR RADYGIN
Moscow State Industrial University of, Science Department
115280, Avtozavodskaya st. 16, Moscow, Russia
bogom-ov@mail.ru

Abstract: The mesoscopic mathematical model of flow in thin channel with rough walls in the 2D approach is proposed. The model is based on the lattice-Bolzmann numerical method. The measured roughness profiles were used in numerical experiments. The effect of the surface roughness upon leakage is shown.
Keywords: *thin channel, surface roughness, Navier-Stokes flow, lattice-Boltzmann*

1. Introduction

Designing of the new mechanical components and technical elements for modern industry often states the problem of providing the desirable hermiticity of thin gaps or regulating the flow through thin channels. Flow pattern in such thin layers significantly determines total efficiency of developed machines and devices.

Main factors, which have a great influence upon the leakage in thin channels of machine components, include interaction characteristics, physico-mechanical properties and geometry of the channel. Roughness of the channel surfaces is also one of the main factors, which have a great impact on leakage.

In authors' earlier works some numerical models of the lubrication flow in the immovable and moving seals with rough walls were proposed [1, 2]. The flow factors were offered for considering the surface roughness effect. The detailed analysis of the surface roughness influence upon the seal hermeticity was presented.

But the lubrication flow model based on the common Reynolds equation is associated with essential restrictions on the physical features of the media and the flow patterns. For example it implies laminar flow with very low Reynolds numbers (Re should not surpass 10–20). Such restrictions significantly shorten the possible range of considerable mechanical components, especially with moving walls.

Present work introduces a new numerical lattice-Boltzmann model of the flow in the thin channels with rough walls. Accepted numerical method allows to turn to the Navier-Stokes approach which has much less physical limitation than lubrication flow approach. So, proposed model allows to examine the influence of the surface roughness upon the flow in the thin channel in Navier-Stokes approach.

2. Mesoscopic flow model

The geometry model of the thin channel formed by two rough surfaces h_1, h_2 is presented in Figure 1. The average gap between two rough surfaces (H) is taken as the distance between their mean lines. Upper and lower walls has coordinates $H_1(x) = H + h_1(x)$ and $H_2(x) = H + h_2(x)$. The current gap in the channel is calculated as $h_T(x) = H + h_1(x) + h_2(x)$.

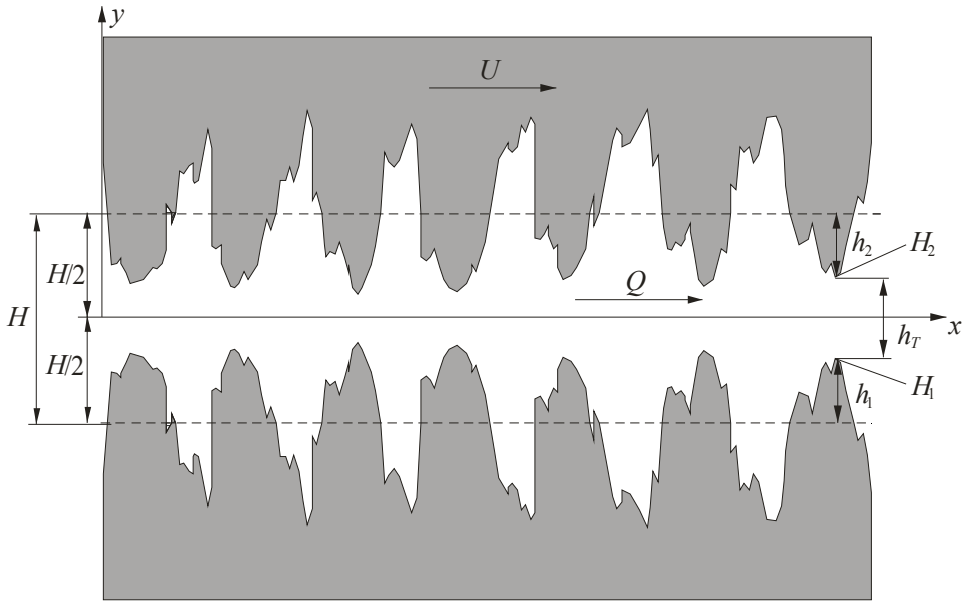


Figure 1. Geometry model of the thin channel with rough walls

Measured profiles of the real industrial surfaces or simulated roughness profiles with desirable features can be used as a surface geometry. Both profiles are always specified on regular grid with Δx step.

For the lattice-Boltzman modelling the square shape numerical lattice δx = δy should be introduced on the channel geometry model. Numerical lattice step is considered as some fraction of the profile grid Δx = kδx where k is an integer value.

The common Navier-Stokes equations are frequently used as a model of viscous flow of a laminar Newtonian media. For the viscous gas in vector notation they are:

$$\rho\frac{du}{dt} = \rho F - grad(p)\left(p + \frac{2}{3}\mu\, div(u)\right) + 2div(\mu S),$$

$$\frac{d\rho}{dt} + \nabla(\rho u) = 0, \qquad (1)$$

where u is the flow velocity, ρ is the media density, p is the pressure, μ is the media viscosity, S is the stress deviation tensor, F represents body forces.

There are three traditional ways of solving the Navier-Stokes equations – finite difference method, finite element method and finite volume method. All traditional methods have some significant problems dealing with curved boundaries.

That is why the alternative lattice methods are widely applied for the flow modelling in modern investigations. They use the representation of the flowing media as a composition of particles interacting on the discrete lattice. Implementation of the fundamental conservation laws, laying in the base of Navier-Stokes equation, guarantees them correct results. Some lattice methods deals with microscopic interactions of single particles in the lattice nodes. Other methods use mesoscopic approach implying the particle distributions in each lattice node.

Lattice-Boltzmann numerical method is a general lattice method based on the mesoscopic Boltzmann transport equation. If we consider f(r, v, t) as a particle distribution by particle velocity v in each r(x, y, z) point at the time moment t, the Boltzmann equation has a form of:

$$f\left(r+vdt, v+Fdt, t+dt\right)dr\,dv - f\left(r,v,t\right)dX\,dv = \Omega(f)\,dr\,dv\,dt \;\Rightarrow$$

$$\frac{\partial f}{\partial t} + \left\| v_x \frac{\partial f}{\partial x} + v_y \frac{\partial f}{\partial y} \right\| + \left\lfloor F_x \frac{\partial f}{\partial v_x} + F_y \frac{\partial f}{\partial v_y} \right\rfloor = \Omega ,$$

$$\Rightarrow \frac{\partial f}{\partial t} + v\frac{\partial f}{\partial r} + F\frac{\partial f}{\partial v} = \Omega(f) , \tag{2}$$

where Ω is the collision operator, characterizing the physical conditions of the media. In 2D case Boltzmann equation is expanded as:

$$\frac{\partial f}{\partial t} + \left\| v_x \frac{\partial f}{\partial x} + v_y \frac{\partial f}{\partial y} \right\| + \left\lfloor F_x \frac{\partial f}{\partial v_x} + F_y \frac{\partial f}{\partial v_y} \right\rfloor = \Omega . \tag{3}$$

Local flow characteristics at each point are calculated by integrating of the particle distribution:

$$\rho(r,t) = \int m\, f(r,v,t)\, dv ,$$

$$\rho(r,t)\,u(xrt) = \int m\, v\, f(r,v,t)\, dv ,$$

$$u(r,t) = \frac{1}{\rho(r,t)} \int m\, v\, f(r,v,t)\, dv ,$$

$$\rho(r,t)e(r,t) = \frac{1}{2}\int m \left\| v-u \right\|^2 f(r,v,t)\, dv ,$$

$$e(r,t) = \frac{1}{2\rho(r,t)} \int m \left\| v-u \right\|^2 f(r,v,t)\, dv \tag{4}$$

where m is generalized particle mass, e is the intrinsic energy. For isothermal flow the e = const condition should be used.

The Bhatnagar-Gross-Kroor (BGK) collision operator is commonly used for simulating the viscous Navier-Stokes flow. It reduces the particle distribution to the equilibrium distribution, defined by Maxwell-Boltzmann equation:

$$f^0(v) = \frac{n}{(2\pi\theta)^{3/2}} exp\left[-(v-u)^2 / 2\theta\right], \tag{5}$$

where $\theta = k_B T = 2e/3$ is the generalized temperature, $n = \rho / m$ is the local particle amount. Simple BGK approximation is a time relaxation operator:

$$\Omega = \frac{1}{\tau}\left(f - f^0\right) , \tag{6}$$

Substituting BGK approximation (6) the Boltzmann equation (3) should be transformed as:

$$\frac{\partial f}{\partial t} + \left\| v_x \frac{\partial f}{\partial x} + v_y \frac{\partial f}{\partial y} \right\| + \left[F_x \frac{\partial f}{\partial v_x} + F_y \frac{\partial f}{\partial v_y} \right] = \frac{1}{\tau}\left(f - f^0\right) \quad (7)$$

As shown in Chapman-Enskog analysis [3], the Boltzmann equation with BGK collision operator (7) is equal to the Navier-Stokes equation (1) for uncompressed fluid or slightly compressed gas when the Mach number is small and the flow is isothermal.

3. Calculation model

According to the numerical lattice-Boltzmann method the calculation process is simulated as a sequential evolution of the flow on the discrete lattice. During the streaming step all particles are migrated to the neighbouring nodes in all possible directions. Particles that appeared in the same node take part into the collision step. Converging iterative process describes the stationary flow behaviour.

In present research the D2Q9 discrete lattice was chosen for the numerical simulations. This lattice assumes migration of particles in 4 straight and 4 diagonal directions as shown in Figure 2. The zero-migration discrete direction (node 9) is also implied.

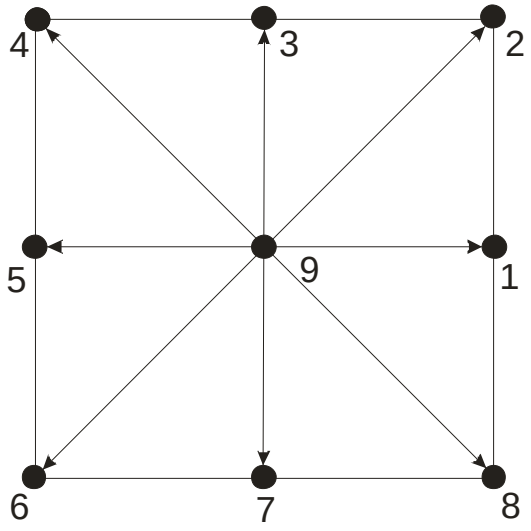


Figure 2. Lattice-Boltzmann D2Q9 numerical lattice

Straight discrete movements implies discrete particle velocities of absolute value $|v_i| = c$ where $c = \delta_x/\delta_t$ is a lattice constant (lattice sound speed) and δ_t is the time step. Diagonal movements implies greater velocities of absolute value $|v_i| = \sqrt{2}c$. The resulting discrete velocity vector is calculated as:

$$v_i = \begin{cases} \left(\cos\left[(i-1)\pi/4\right], \sin\left[(i-1)\pi/4\right]\right)c, & i = 1,3,5,7 \\ \left(\cos\left[(i-1)\pi/4\right], \sin\left[(i-1)\pi/4\right]\right)\sqrt{2}c, & i = 2,4,6,8 \\ (0,0), & i = 9 \end{cases}. \tag{8}$$

The continuous particle distribution function is also substituted by a set of discrete distribution functions:

$$f(r, v_i, t = f_i(r,t)). \tag{9}$$

The streaming step is simulated as:

$$f_i(r + v_i\delta_x, t + \delta_t) = f_i(r,t) - F_i. \tag{10}$$

The collision step equation can be expanded from the continuous Boltzmann equation with BGK approximation (7):

$$f_i'(r, t+\delta_t) = f_i(r, t+\delta_t) + \frac{1}{\tau_\delta}\left[f^0(\rho, u, \theta) - f_i(r, t+\delta_t)\right], \tag{11}$$

where $\tau_\delta = \tau/\delta_x$ is the discrete relaxation parameter, f' is the new particle distribution after the collision step. Local quantities

Local flow characteristics implicated in the equation (11) in discrete form are calculated by transforming integral to sum:

$$n = \sum_i f_i, \quad \rho = m\sum_i f_i, \quad u = \frac{m\sum_i v_i f_i}{\sum_i v_i f_i}. \tag{12}$$

Discrete equilibrium particle distribution for the isothermal flow is calculated as shown in [3, 4]:

$$f_i^0 = nw_i\left[1 + \frac{3}{c^2}v_i \cdot u + \frac{9}{2c^4}(v_i \cdot u)^2 - \frac{3}{2c^2}u \cdot u\right], \tag{13}$$

where w_i are the specific weight coefficients. For the D2Q9 lattice they are defined as:

$$w_i = \begin{cases} \frac{1}{9}, & i = 1, 3, 5, 7, \\ \frac{1}{36}, & i = 2, 4, 6, 8, \\ \frac{4}{9}, & i = 9. \end{cases} \tag{14}$$

The local conservation laws are also true for the equilibrium distribution:

$$m\sum_i f_i^0 = \rho, \quad m\sum_i v_i f_i^0 = \rho u \tag{15}$$

While using numerical lattice methods, standard macroscopic boundary conditions should be converted to the mesoscopic terms (specific particle distributions and collision operators on the boundaries).

For the solid wall boundaries of the channel the no-flow and no-slip macroscopic boundary conditions should be implemented. As a mesoscopic alternative, the classic "bounce-back" boundary scheme [4] was used in present research. In "bounce-back" boundary nodes are not the part of the flow and special collision operator is defined them. All the particles, arrived to the boundary node on the streaming step are just mirrored in the opposite directions on the collision step:

$$f_{i^*}'(r_b, t+\delta_t) = f_i(r_b, t+\delta_t), \tag{16}$$

where r_b means boundary node coordinates, i* is the direction opposite to i direction.

For the open boundaries of the channel there are two ways of defining boundary conditions. The first way is to define flow velocity boundary conditions:

$$u = Const = u_I \text{ on the channel inlet,}$$
$$\partial u / \partial \hat{x} = 0 \text{ on the channel outlet.} \tag{17}$$

Here is the mesoscopic interpretation of flow velocity boundary conditions:

$$f_{i^*}'(r_I,\ t+\delta_t) = f_i(r_I + v_{i^*}\delta_t,\ t+\delta_t) + 2w_{i^*}\rho\left(r_I + v_{i^*}\delta_t\right)\frac{3}{c^2}\left(v_{i^*} \cdot u_I\right)$$
$$f_i'(r_O,\ t+\delta_t) = f_i(r_f,\ t+\delta t). \tag{18}$$

where r_I is the inlet boundary node, r_O is the outlet boundary node, r_f is a flow node adjacent to the r_O.

The second way is to define strict p boundary conditions:

$$p = p_I \text{ on the channel inlet,}$$
$$p = p_O \text{ on the channel outlet.} \tag{19}$$

On the mesoscopic level constant pressure on the boundaries means constant ρ because $p = c_s^2\rho$. The equilibrium particle distributions with zero velocity are used for boundary conditions:

$$f_i = \frac{p_B w_i}{m c_s^2}. \tag{20}$$

where p_B is the pressure on the specified open boundary node.

After the lattice-Boltzmann calculation is finished the resulting local flow characteristics could be calculated by (12). Then the integrated flow characteristics could be calculated.

Total leakage through the channel was calculated as an integrated horizontal velocity of the local flow on the channel outlet:

$$Q_x = B\sum_{j=1}^{J} u_x(L, y_j)\delta_x \tag{21}$$

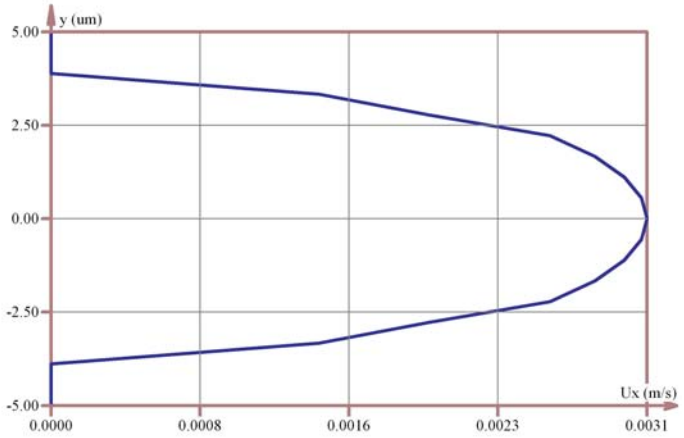
where B is the channel thickness, L is the channel length.

The flow factor φ_x was also calculated, that shows the decrease of Q_x in comparison to the smooth wall channel with the same geometry Q_x*:

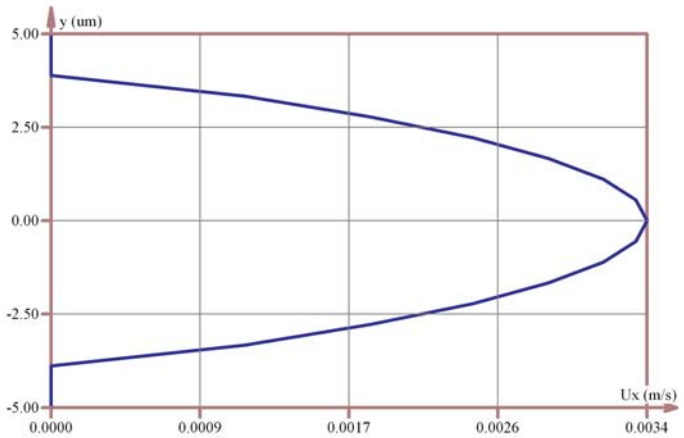
$$Q_x^* = \frac{B H^3 (p_A - p_B)}{12\mu L}, \quad \varphi_x = Q_x / Q_x^*. \tag{22}$$

4. Analysis

The computation software were developed for the proposed numerical model and the numerical experiments were carried out. The results achieved for the smooth wall channel are shown in Figure 3.



near open boundaries



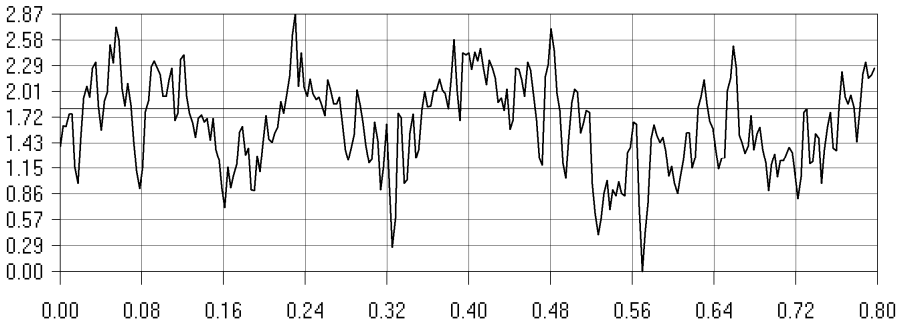
inner section

Figure 3. Vertical section of u_x for channel width smooth walls

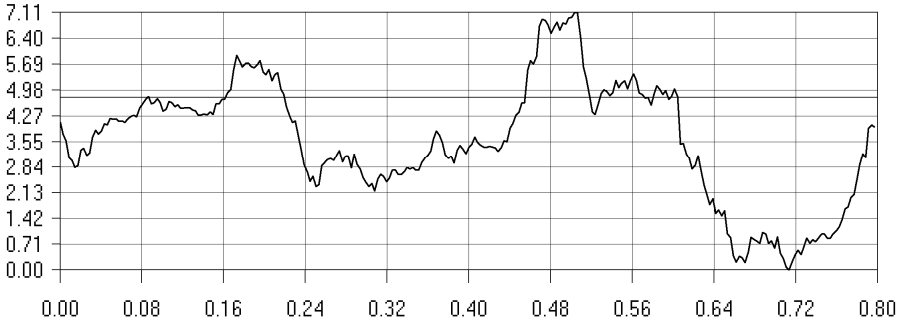
The well-known feature of the flow in the smooth wall channel is a parabolic distribution of flow velocity in the vertical section of the channel. Strict parabolic distribution was achieved in LBM simulation for the inner sections of the channel. Some transient process was achieved near the open boundaries. They are due to the constant boundary conditions on open boundaries. The other well-known features of the flow in the

smooth wall channel (negligible vertical pressure gradient and vertical velocity, linear pressure distribution along the channel length) were also granted in numerical simulations. In complex they validate the numerical model correctness.

Other numerical experiments were carried out for the rough wall channels. In Figure 4 two different rough surfaces are shown. The first one is the surface after the grinding with low roughness height. The second one is the surface after milling with greater roughness height. The length of the analysed channel was 0,8 mm.



surface after grinding

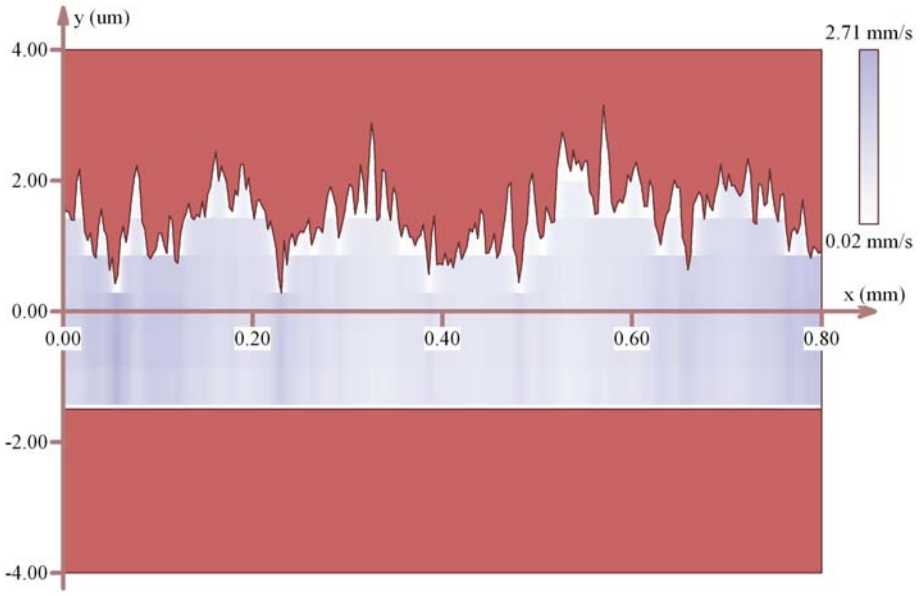


surface after milling

Figure 4. Surface roughness profiles

Typical flow velocity distribution in channels with both grinded and milled surfaces is shown in Figure 5. The local velocity significantly increases where the channel is narrowed. In vertical section the flow velocity still has parabolic distribution. Also the increase of vertical flow velocity near the channel narrowing zones was achieved. It is due to the streamlining of the roughness peaks.

The resulting values of the flow factors in channel with different surface roughness profiles are shown in Figure 6. The results are shown as a graph showing the flow factor evolution while growing of the average gap from 7 to 12 um. For the more thin channels the flow factor values are more significant, i.e. the roughness influence is more strong. Regular surfaces with great roughness height show stronger influence.



surface after grinding



surface after milling

Figure 5. Flow velocity in channels with rough walls

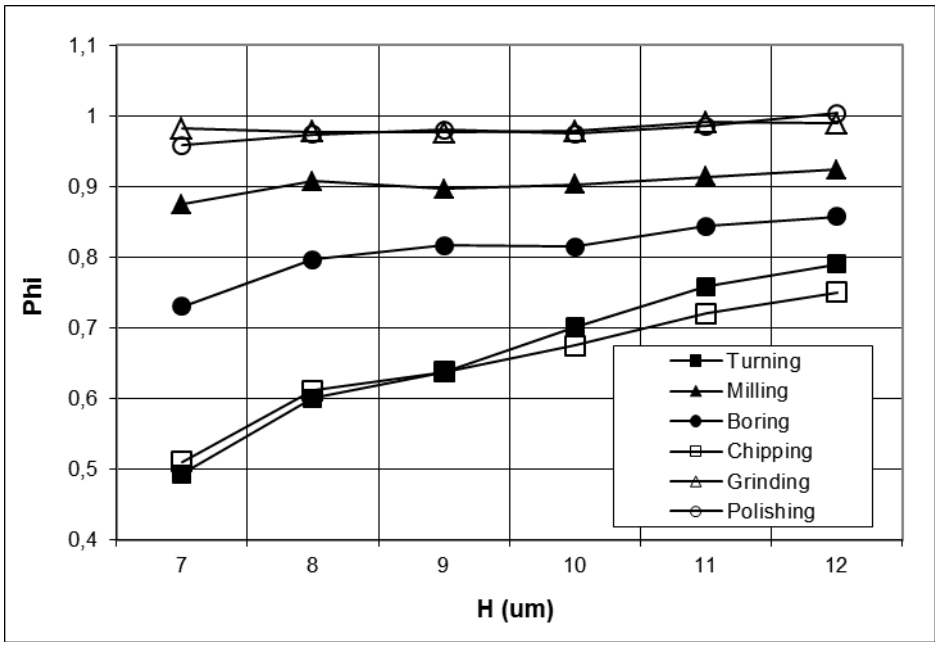


Figure 6. Evolution of the flow factors with growing of average gap H

At the same time, the small roughness surfaces allow to achieve lesser values of average gap and so decrease leakages.

5. Conclusion

Proposed model can be used to forecast leakage in thin channels with rough walls in the Navier-Stokes approach. Small roughness height should be combined with regular surface texture to decrease the resulting leakage.

The research was performed with the financial support of the Ministry of Education and Science of the Russian Federation for higher education institutions within the state job service.

6. References

[1] Poroshyn, V. V.–Bogomolov, D. G.: Application of finite element method (FEM) for calculation of flow factors in seals. *International Journal of Applied Mechanics and Engineering,* 2002, Vol. 7, No. 3, pp. 961–972.

[2] Shejpak, A.–Poroshin, V.–Syromiatnikova, A.–Bogomolov, D.: Roughness influence upon the hermiticity of plunged pair using equivalent gap model. *Advanced Engineering,* (2008) No. 2, pp. 283–290.

[3] Wagner, A. J. *A practical introduction to the Lattice Boltzmann method.* North Dakota State University, 2008.

[4] Mei, R.–Luo, L. S.–Shyy, W.: *An accurate curved boundary treatment in the Lattice-Boltzmann method.* ICASE report No 2000-6. Langley Research Center, 2000.